Approximating the shifted Hartree-exchange-correlation potential in direct energy Kohn-Sham theory

Daniel J. Sharpe,[†] Mel Levy,[‡] and David J. Tozer[*,†]

[†]*Department of Chemistry, Durham University, South Road, Durham, DH1 3LE UK*

[‡]*Department of Chemistry, Duke University, Durham, North Carolina 27708 USA; Department of Physics, North Carolina A&T State University, Greensboro, North Carolina 27411 USA; Department of Chemistry and Quantum Theory Group, Tulane University, New Orleans, Lousiana 70118 USA*

E-mail: d.j.tozer@durham.ac.uk

Abstract

Levy and Zahariev [Phys. Rev. Lett. **113** 113002 (2014)] have proposed a new approach for performing density functional theory calculations, termed direct energy Kohn-Sham (DEKS) theory. In this approach, the electronic energy equals the sum of orbital energies, obtained from Kohn-Sham-like orbital equations involving a shifted Hartree-exchange-correlation potential, which must be approximated. In the present study, density scaling homogeneity considerations are used to facilitate DEKS calculations on a series of atoms and molecules, leading to three non-local approximations to the shifted potential. The first two rely on preliminary Kohn-Sham calculations using a standard generalised gradient approximation (GGA) exchange-correlation functional and the results illustrate the benefit of describing the dominant Hartree component of the shift exactly. A uniform electron gas analysis is subsequently used to eliminate the

need for these Kohn-Sham calculations, leading to a potential with an unconventional form that yields encouraging results, providing strong motivation for further research in DEKS theory.

1 Introduction and Background

In density functional theory (DFT), the ground state electronic energy (omitting nuclear repulsion) is

$$E = T_{\rm s} + \int v(\mathbf{r})\rho(\mathbf{r})d\mathbf{r} + G\,, \tag{1}$$

where $T_{\rm s}$ is the non-interacting kinetic energy, $v(\mathbf{r})$ is the external potential, $\rho(\mathbf{r})$ is the ground state electron density, and G is the Hartree-exchange-correlation (Hxc) energy,

$$G = J + E_{\rm xc}\,, \tag{2}$$

comprising the Hartree energy,

$$J = \frac{1}{2}\int\int \frac{\rho(\mathbf{r})\rho(\mathbf{r}')}{|\mathbf{r}-\mathbf{r}'|}d\mathbf{r}d\mathbf{r}'\,, \tag{3}$$

and the exchange-correlation energy, $E_{\rm xc}$.

In Kohn-Sham (KS)[1] DFT, the density is obtained from orbitals, $\varphi_i(\mathbf{r})$, that are solutions to the KS equations,

$$\left[-\frac{1}{2}\nabla^2 + v(\mathbf{r}) + w(\mathbf{r})\right]\varphi_i(\mathbf{r}) = \epsilon_i\varphi_i(\mathbf{r})\,, \tag{4}$$

where $w(\mathbf{r})$ is the Hxc potential,

$$w(\mathbf{r}) = \frac{\delta G}{\delta\rho(\mathbf{r})} = v_J(\mathbf{r}) + v_{\rm xc}(\mathbf{r})\,, \tag{5}$$

comprising Hartree and exchange-correlation potentials, respectively, and ϵ_i are the orbital energies. Multiplying Eq (4) on the left by $\varphi_i(\mathbf{r})$, summing over occupied orbitals i, integrating over space, and using the definition of the density, allows Eq (1) to be re-written as

$$E = \sum_i \epsilon_i + G - \int w(\mathbf{r})\rho(\mathbf{r})d\mathbf{r}\,, \tag{6}$$

illustrating that the KS electronic energy is not the sum of the orbital energies.

In a recent study, Levy and Zahariev (LZ)[2] proposed an alternative formalism where the electronic energy is the sum of the orbital energies. They considered the Kohn-Sham-like equations,

$$\left[-\frac{1}{2}\nabla^2 + v(\mathbf{r}) + \overline{w}(\mathbf{r})\right]\varphi_i(\mathbf{r}) = \overline{\epsilon}_i\varphi_i(\mathbf{r})\,, \tag{7}$$

where $\overline{w}(\mathbf{r})$ is a shifted Hxc potential,

$$\overline{w}(\mathbf{r}) = w(\mathbf{r}) + c\,, \tag{8}$$

and c is the density-dependent constant shift,

$$c = \frac{G - \int w(\mathbf{r})\rho(\mathbf{r})d\mathbf{r}}{N}\,, \tag{9}$$

where

$$N = \int \rho(\mathbf{r})d\mathbf{r} \tag{10}$$

is the electron number. The orbital solutions to Eq (7) are the KS orbitals, but the orbital energies $\overline{\epsilon}_i$ are shifted from the KS orbital energies by c. In analogy to the KS case, the

electronic energy in Eq (1) can be re-written as

$$E = \sum_i \overline{\epsilon}_i + G - \int \overline{w}(\mathbf{r})\rho(\mathbf{r})d\mathbf{r}\,. \tag{11}$$

However, it follows from Eqs (8) and (9) that

$$G = \int \overline{w}(\mathbf{r})\rho(\mathbf{r})d\mathbf{r} \tag{12}$$

and so Eq (11) reduces to the desired result,

$$E = \sum_i \overline{\epsilon}_i\,. \tag{13}$$

In practical calculations, Eqs (4) and (7) must be solved within a finite basis set, but this does not affect the form of Eqs (6) and (13).

LZ showed that the exact potential $\overline{w}(\mathbf{r})$ has desirable characteristics. First, it does not exhibit a discontinuity[3] upon an increase in fractional electron number[3–6] beyond an integer. This is evident from Eq (13): the exact electronic energy must be continuous with electron number, which requires the sum of the orbital energies and thus the potential, $\overline{w}(\mathbf{r})$, to be continuous. And second, it can be shown that upon any isoelectronic change in the density, $\overline{w}(\mathbf{r})$ changes less than any other potential that differs from $w(\mathbf{r})$ by a density-dependent additive constant. LZ suggested that approximating $\overline{w}(\mathbf{r})$ directly − and subsequently solving Eq (7) and calculating the electronic energy using Eq (13) − represents a new, direct energy Kohn-Sham (DEKS) approach for approximating the ground state density and energy in DFT. The practical value of such a scheme will depend on how well $\overline{w}(\mathbf{r})$ can be approximated; any insight that can be provided will be valuable. For further discussion of the DEKS approach, see Refs 2,7–11; also see Refs. 12,13 for an earlier, Hartree-Fock variant.

The key quantities in DFT are functionals of the density and in another series of papers,[14–20] Tozer and co-workers have studied their density scaling properties. A functional

$F[\rho]$ is said to be homogeneous of degree k_F under density scaling if it satisfies

$$F[\lambda\rho] = \lambda^{k_F} F[\rho]\,, \tag{14}$$

or equivalently (for $k_F \neq 0$),[21]

$$k_F = \frac{\int \frac{\delta F}{\delta\rho(\mathbf{r})}\rho(\mathbf{r})d\mathbf{r}}{F}\,. \tag{15}$$

As an example, the Dirac exchange[22] functional is homogeneous of degree 4/3 under density scaling.

For an arbitrary functional F, Eq (15) can be regarded[23] as *defining* a homogeneity parameter, k_F, that quantifies the behaviour of that functional under density scaling. If the value of k_F evaluated using Eq (15) is the same for all systems then the functional is homogeneous. However, if the value is system-dependent then the functional is inhomogeneous and the degree of system-dependence provides a measure of the degree of inhomogeneity. Using these ideas, the KS electronic energy in Eq (6) can be written

$$E = \sum_i \epsilon_i + G(1 - k_G) \tag{16}$$

where k_G is the homogeneity parameter for the Hxc functional,

$$k_G = \frac{\int \frac{\delta G}{\delta\rho(\mathbf{r})}\rho(\mathbf{r})d\mathbf{r}}{G} = \frac{\int w(\mathbf{r})\rho(\mathbf{r})d\mathbf{r}}{G}\,. \tag{17}$$

It is evident from Eq (16) that if the homogeneity parameter was to take the value $k_G = 1$, then the KS electronic energy would reduce to the sum of the orbital energies, thereby highlighting a key link between density scaling behaviour and the DEKS approach. The aim of the present study is to use density scaling homogeneity considerations to facilitate DEKS calculations and to provide approximations to the shifted potential, $\overline{w}(\mathbf{r})$.

We commence in Section 2 by defining our Hxc functional and shifted potential and describing our computational procedure for performing DEKS calculations. Attention is paid to the partitioning of the shifted potential into Hartree and exchange-correlation components and the calculation of reference data to compare with. DEKS results are presented in Section 3. Initially, we present results based on the use of $k_G = 1$, using input from preliminary KS calculations with a standard generalised gradient approximation (GGA) exchange-correlation functional. Examination of the potentials leads us to modify the approach, in order to describe the dominant Hartree component of the shift exactly. Significant improvements are obtained, although the calculations still rely on preliminary KS calculations. A uniform electron gas analysis is used to eliminate this reliance, leading to a potential with an unconventional form that yields encouraging results. Conclusions are presented in Section 4.

2 Methodology

2.1 Functional form and computational procedure

We start by defining an underlying Hxc functional (Eq (2)), the potential of which will be shifted by c to yield the desired $\overline{w}(\mathbf{r})$ in Eq (8). For the Hartree component, we use the exact J in Eq (3), which is homogeneous of degree two under density scaling (i.e. Eq (15) yields $k_J = 2$). For the exchange-correlation component, we write

$$E_{\rm xc} = \alpha G_{\rm xc}\,, \tag{18}$$

where α is a parameter and

$$G_{\rm xc} = \Big(\int \rho^{\frac{3k}{3k-1}}(\mathbf{r}) d\mathbf{r} \Big)^{\frac{3k-1}{3}}\,. \tag{19}$$

This exchange-correlation functional, which is based on a form proposed by Liu and Parr,[24] is homogeneous of degree k under density scaling (i.e. Eq (15) yields $k_{\rm xc} = k$). With respect to

the more common coordinate scaling,[25] it is homogeneous of degree one, which is motivated by the fact that the exact exchange component behaves in this manner. Our Hxc functional is therefore

$$G = J + \alpha G_{\rm xc}\,. \tag{20}$$

Next, we define the values of c (Eq (9)) and k (in Eq (19)); see later for details. The value of α in Eq (20) is then determined. Initially, in Sections 3.1 and 3.2, we determine it on a system-by-system basis (using similar ideas to those of Ref. 20) by performing a preliminary KS calculation using a standard GGA exchange-correlation functional and requiring that the evaluation of the approximate G in Eq (20), using the GGA density, yields the GGA Hxc energy. This simply requires

$$\alpha = E_{\rm xc}^{\rm GGA}/G_{\rm xc}^{\rm GGA}\,, \tag{21}$$

where $G_{\rm xc}^{\rm GGA}$ is obtained by evaluating Eq (19) using the GGA density and $E_{\rm xc}^{\rm GGA}$ is the GGA exchange-correlation energy. For the GGA, we use the Perdew-Burke-Ernzerhof (PBE) functional[26] throughout. In Section 3.4, an alternative approach for determining α is used, which does not rely on a preliminary KS calculation.

We then construct the potential $\overline{w}(\mathbf{r})$ in Eq (8) for our Hxc functional in Eq (20),

$$\overline{w}(\mathbf{r}) \;\; = \;\; v_J(\mathbf{r}) + \alpha\frac{\delta G_{\rm xc}}{\delta\rho(\mathbf{r})} + c\,, \tag{22}$$

where

$$\frac{\delta G_{\rm xc}}{\delta\rho(\mathbf{r})} = k\Big(\int \rho^{\frac{3k}{3k-1}}(\mathbf{r})d\mathbf{r}\Big)^{\frac{3k-4}{3}}\rho^{\frac{1}{3k-1}}(\mathbf{r})\,, \tag{23}$$

noting that α simply contributes a multiplicative factor because it is constructed from the

fixed, GGA density. It is noteworthy that, like the Hartree potential, $v_J(\mathbf{r})$, the potential in Eq (23) is non-local, in the sense that its value at a point in space depends on the electron density at all points in space.

We then solve the DEKS orbital equations (7) within the basis set, using the potential in Eq (22), and evaluate the electronic energy using Eq (13); the value must be identical to that obtained using the conventional evaluation, Eq (1).

The variational nature of our DEKS implementation was verified with the usual Hellmann-Feynman dipole moment check. We consider 17 closed-shell atoms and small molecules, taken from Ref. 15, namely He, Be, Ne, Mg, Ar, CH_4, NH_3, H_2O, HF, CO, N_2, F_2, PH_3, H_2S, HCl, SO_2, and Cl_2. All calculations are performed using the aug-cc-pVTZ basis set at the reference, near-exact geometries of Ref. 27, using the CADPAC program.[28]

2.2 Partitioning of the shifted Hxc potential

In addition to the total potential, $\overline{w}(\mathbf{r})$, it is of interest to consider the individual Hartree and exchange-correlation components. For a general DEKS calculation, it follows from Eqs (2) and (5) that the shift in Eq (9) partitions into

$$c = c_J + c_{\rm xc} \,. \tag{24}$$

The Hartree component is

$$c_J = \frac{J - \int v_J(\mathbf{r})\rho(\mathbf{r})d\mathbf{r}}{N} = -\frac{J}{N} \,, \tag{25}$$

where we have used the fact that J is homogeneous of degree two under density scaling. Similarly, the exchange-correlation component is

$$c_{\rm xc} = \frac{E_{\rm xc} - \int v_{\rm xc}(\mathbf{r})\rho(\mathbf{r})d\mathbf{r}}{N} \,. \tag{26}$$

The total potential in Eq (8) can therefore be partitioned as

$$\overline{w}(\mathbf{r}) = \overline{v}_J(\mathbf{r}) + \overline{v}_{\rm xc}(\mathbf{r}), \tag{27}$$

where

$$\overline{v}_J(\mathbf{r}) = v_J(\mathbf{r}) + c_J \tag{28}$$

and

$$\overline{v}_{\rm xc}(\mathbf{r}) = v_{\rm xc}(\mathbf{r}) + c_{\rm xc}\,. \tag{29}$$

It follows from Eqs (25), (26), (28), and (29) that the individual energy components are simply expressed in terms of these potentials,

$$J = \int \overline{v}_J(\mathbf{r})\rho(\mathbf{r})d\mathbf{r} \tag{30}$$

and

$$E_{\rm xc} = \int \overline{v}_{\rm xc}(\mathbf{r})\rho(\mathbf{r})d\mathbf{r}\,, \tag{31}$$

in a manner analogous to Eq (12).

We therefore partition our potential in Eq (22) according to Eq (27), noting that the specific form of the exchange-correlation component is

$$\overline{v}_{\rm xc}(\mathbf{r}) = \alpha\frac{\delta G_{\rm xc}}{\delta\rho(\mathbf{r})} + c_{\rm xc}\,. \tag{32}$$

The value of c_J is obtained by evaluating Eq (25) using the self-consistent density. The value of $c_{\rm xc}$ can be obtained by substituting Eq (18) into Eq (26) but, as will be seen, this is not

necessary in practice because the value of $c_{\rm xc}$ is completely determined by our choice of c.

2.3 PBE DEKS results for comparison

Given the role of the PBE GGA functional in our computational approach, it is natural to quantify the accuracy of our DEKS results by comparing with DEKS results obtained using PBE. The latter are straightforward to perform: We solve the KS equations (4) within the basis set using PBE and then compute the shift c, either directly using Eq (9) or, given that the electronic energy is already known, by simply rearranging Eqs (6) and (9) to give

$$c = \frac{E - \sum_i \epsilon_i}{N} \,. \tag{33}$$

We then determine c_J by evaluating Eq (25) using PBE quantities and evaluate $c_{\rm xc}$ using Eq (24). The PBE DEKS $\bar{\epsilon}_i$ values are then obtained by adding c to the KS orbital energies. The PBE DEKS electronic energies (Eq (13)) and exchange-correlation energies (Eq (31)) are identical to the KS values, whilst the PBE DEKS potentials comprise the KS potentials, shifted by c_J and $c_{\rm xc}$.

We note that for the 17 systems considered, the PBE c_J values are significantly larger in magnitude, and opposite in sign, to the $c_{\rm xc}$ values. Specifically, the average value of the ratio $c_J/c_{\rm xc}$ is -20.3, which can be understood in part from the fact that PBE is approximately homogeneous of degree 4/3 under density scaling (the dominant component is Dirac exchange). It follows from Eqs (26) and (15) that for PBE,

$$c_{\rm xc} \approx \frac{E_{\rm xc} - \frac{4}{3}E_{\rm xc}}{N} \approx -\frac{E_{\rm xc}}{3N} \,. \tag{34}$$

and so from Eqs (25) and (34), $c_J/c_{\rm xc} \approx 3J/E_{\rm xc}$. The average value of this ratio for the 17 systems is -17.6, close to the aforementioned value.

3 Results

3.1 DEKS calculations using $k_G = 1$ ($c = 0$, $c_{\mathbf{xc}} = -c_J$)

Our initial investigations centred around the aforementioned observation that if $k_G = 1$ then the KS electronic energy equals the sum of the orbital energies. Given that the role of the shift, c, in DEKS is to shift the KS Hxc potential to achieve exactly this, it follows that c must be zero (i.e. DEKS $\equiv$ KS) and this is easily verified by evaluating Eq (9) using Eq (17) with $k_G = 1$. It follows from Eq (24) that $c_{\text{xc}} = -c_J$. We therefore commence by performing DEKS calculations with $k_G = 1$, $c = 0$, $c_{\text{xc}} = -c_J$. It is important to note that setting $c = 0$ does not preclude a shift in the potential compared to the KS potentials of conventional functionals; it simply means that any shift must be directly incorporated into the potential via the functional form, rather than being explicitly added.

Evaluating the homogeneity parameter, Eq (17), for the functional G in Eq (20) yields

$$k_G = \frac{2J + k\alpha G_{\text{xc}}}{J + \alpha G_{\text{xc}}} \tag{35}$$

and so setting $k_G = 1$ yields the value of k to be used in Eq (19),

$$k = 1 - \frac{J}{\alpha G_{\text{xc}}}\,. \tag{36}$$

We determine this value on a system-by-system basis by approximating J to be the KS GGA Hartree energy and αG_{xc} to be the KS GGA exchange-correlation energy, from preliminary KS calculations. We then follow the procedure described in Section 2.1, using $c = 0$ and Eq (21). However, due to the use of GGA quantities in the calculation of k, the value of k_G determined using the self-consistent DEKS quantities is not exactly unity and so the electronic energy in Eq (1) is not exactly equal to the sum of the orbital energies. Discrepancies range from 0.01 a.u. (He) to 24.32 a.u. (Cl_2), with an average discrepancy across the 17 systems of 6.34 a.u. These discrepancies are significantly smaller than from

PBE KS calculations (1.73 a.u. (He) to 465.85 a.u. (Cl_2), with an average of 127.98 a.u.), but they are still non-negligible and the calculations are not true DEKS calculations.

To address this, we use the values of J and $\alpha G_{\rm xc}$ from the initial DEKS calculation to determine a revised value of k using Eq (36) and then repeat the procedure in Section 2.1. Iterating this whole process leads to computed k_G values that do approach unity and electronic energies in Eq (1) that do approach the sum of the orbital energies. In practice, we stop the iterative procedure when the electronic energy agrees with the sum of the orbital energies to within one milihartree, which is orders of magnitude smaller than the aforementioned discrepancies. For the systems considered, this is achieved after two to four iterations (two iterations for He; three iterations for the other systems not containing third row atoms; and four iterations for systems containing third row atoms). The results are denoted DEKS1.

Table 1 presents the DEKS1 k and α values for the 17 systems, ordered by increasing electron number, N. With increasing N, the values of k broadly increase, whereas the values of α become less negative, approaching extremely small values. (This can be understood from the fact that as k increases, so the functional in Eq (19) increasingly resembles N^k, thus requiring a very small prefactor). Tables 2, 3, and 4 present the DEKS1 electronic energies (Eq (13) = Eq (1)), exchange-correlation energies (Eq (18) = Eq (31)), and highest occupied molecular orbital (HOMO) energies, $\overline{\epsilon}_{\rm HOMO}$ (from Eq (7)), respectively, compared to the reference PBE DEKS values. The mean absolute deviations (MADs), relative to the PBE DEKS values, are 0.729, 1.927, and 0.170 a.u., respectively. Recall that whilst the PBE DEKS electronic energies and exchange-correlation energies are identical to the KS values, the values of $\overline{\epsilon}_{\rm HOMO}$ are shifted from the KS values by the PBE values of c. These shifts are significant: for the 17 systems, the average value of c is -6.895 a.u. (Put another way, the MAD between PBE KS and PBE DEKS HOMO energies is 6.895 a.u.). The DEKS1 MAD of just 0.170 a.u. in Table 4 suggests that the shift has been successfully incorporated into the potential in the regions of space relevant to the HOMO.

To investigate this, Figures 1(a), 1(b), and 1(c) plot the potentials $\overline{v}_J(\mathbf{r})$, $\overline{v}_{\rm xc}(\mathbf{r})$, and

Table 1: Parameters defining DEKS1, DEKS2, and DEKS3.

	DEKS1		DEKS2	DEKS3
	k	α	α	$\beta N^{\frac{1}{3}}$
He	2.927	-3.210×10^{-01}	-1.046	-0.868
Be	3.566	-5.449×10^{-02}	-1.156	-1.093
Ne	6.195	-1.501×10^{-05}	-1.527	-1.484
CH_4	5.690	-4.954×10^{-05}	-1.544	-1.484
NH_3	5.801	-3.874×10^{-05}	-1.522	-1.484
H_2O	5.920	-2.932×10^{-05}	-1.515	-1.484
HF	6.052	-2.135×10^{-05}	-1.517	-1.484
Mg	6.610	-2.434×10^{-06}	-1.576	-1.577
CO	6.394	-1.797×10^{-06}	-1.722	-1.660
N_2	6.387	-1.826×10^{-06}	-1.726	-1.660
Ar	8.217	-2.844×10^{-09}	-1.734	-1.805
F_2	7.110	-6.217×10^{-08}	-1.860	-1.805
PH_3	7.726	-1.226×10^{-08}	-1.718	-1.805
H_2S	7.913	-7.075×10^{-09}	-1.720	-1.805
HCl	8.072	-4.398×10^{-09}	-1.726	-1.805
SO_2	8.994	-3.519×10^{-12}	-2.151	-2.187
Cl_2	9.219	-1.046×10^{-12}	-2.153	-2.231

Table 2: DEKS electronic energies (in a.u.).

	DEKS1	DEKS2	DEKS3	PBE
He	-2.899	-2.893	-2.718	-2.892
Be	-14.735	-14.643	-14.497	-14.629
Ne	-129.198	-128.906	-128.562	-128.853
CH_4	-40.635	-40.508	-40.243	-40.464
NH_3	-56.749	-56.562	-56.365	-56.512
H_2O	-76.674	-76.434	-76.248	-76.381
HF	-100.728	-100.447	-100.213	-100.393
Mg	-200.740	-199.993	-199.999	-199.949
CO	-113.653	-113.292	-112.800	-113.233
N_2	-109.847	-109.508	-108.991	-109.452
Ar	-528.690	-527.433	-528.691	-527.338
F_2	-199.961	-199.503	-198.902	-199.418
PH_3	-344.100	-343.075	-344.296	-342.988
H_2S	-400.469	-399.324	-400.608	-399.234
HCl	-461.955	-460.728	-462.024	-460.636
SO_2	-549.858	-548.538	-549.235	-548.391
Cl_2	-922.302	-920.185	-922.212	-920.036
MAD vs. PBE	0.729	0.069	0.658	

Table 3: DEKS exchange-correlation energies (in a.u.)

	DEKS1	DEKS2	DEKS3	PBE
He	−1.081	−1.049	−0.840	−1.046
Be	−3.002	−2.717	−2.556	−2.719
Ne	−13.482	−12.270	−11.907	−12.368
CH_4	−7.330	−6.838	−6.553	−6.836
NH_3	−8.639	−7.921	−7.711	−7.946
H_2O	−10.120	−9.184	−8.987	−9.238
HF	−11.756	−10.635	−10.387	−10.713
Mg	−18.205	−16.146	−16.151	−16.290
CO	−14.941	−13.705	−13.184	−13.756
N_2	−14.680	−13.534	−12.987	−13.572
Ar	−34.105	−30.465	−31.749	−30.662
F_2	−22.230	−20.427	−19.793	−20.553
PH_3	−26.876	−23.988	−25.243	−24.142
H_2S	−29.263	−26.040	−27.353	−26.203
HCl	−31.693	−28.197	−29.521	−28.377
SO_2	−46.535	−42.267	−42.986	−42.546
Cl_2	−61.832	−55.711	−57.779	−56.039
MAD vs. PBE	1.927	0.113	0.626	

Table 4: DEKS HOMO energies, $\bar{\epsilon}_{\mathrm{HOMO}}$ (in a.u.)

	DEKS1	DEKS2	DEKS3	PBE
He	−1.449	−1.447	−1.359	−1.446
Be	−1.804	−1.817	−1.804	−1.810
Ne	−6.966	−6.592	−6.574	−6.716
CH_4	−3.566	−3.362	−3.349	−3.436
NH_3	−4.055	−3.843	−3.834	−3.914
H_2O	−4.853	−4.577	−4.568	−4.667
HF	−5.823	−5.491	−5.480	−5.600
Mg	−7.415	−7.818	−7.818	−7.751
CO	−5.645	−5.440	−5.424	−5.505
N_2	−5.640	−5.386	−5.369	−5.462
Ar	−12.987	−12.692	−12.715	−12.737
F_2	−7.446	−7.084	−7.067	−7.201
PH_3	−9.488	−9.422	−9.445	−9.422
H_2S	−10.544	−10.398	−10.420	−10.404
HCl	−11.738	−11.501	−11.523	−11.528
SO_2	−11.248	−11.002	−11.010	−11.057
Cl_2	−14.169	−13.947	−13.965	−13.970
MAD vs. PBE	0.170	0.056	0.065	

$\overline{w}(\mathbf{r})$, respectively (Eqs (27)-(29)), along the bond axis in the representative N_2 molecule, from DEKS1 and PBE DEKS calculations. The nuclei are located at ± 1.037 a.u. Note the different vertical scales on the plots, which have been chosen to capture the key features of the PBE DEKS potentials. The Hartree potentials in Figure 1(a) differ only because of the different densities used in their evaluation; the differences are most pronounced in asymptotic (large $|z|$) regions where the values approach $c_J = -5.65$ a.u. for DEKS1 and $c_J = -5.36$ a.u. for PBE. The exchange-correlation potentials in Figure 1(b) are notably different and this is reflected in the total potentials in Figure 1(c). Note that the PBE behaviour at the nuclei is unphysical, which is a well-known issue with GGA potentials.[29] For this system, the value of the PBE shift is $c = -5.09$ a.u, so it is evident from Figure 1(c) that this shift has been very successfully incorporated into the DEKS1 potential in regions of space relevant to the HOMO, as was anticipated based on the HOMO values in Table 4.

To improve the agreement between the DEKS1 and PBE potentials in Figures 1(a)-(c), the discrepancies in Figure 1(b) must be eliminated; discrepancies in Figures 1(a) and 1(c) will both be eliminated if that can be achieved. It is therefore important to understand the discrepancies in Figure 1(b). The PBE potential is the asymptotically vanishing KS potential, shifted by the relatively small positive amount, $c_{\rm xc} = 0.28$ a.u. For DEKS1, where $c_{\rm xc} = -c_J$, the potential, Eq (32), is

$$\overline{v}_{\rm xc}(\mathbf{r}) = \alpha \frac{\delta G_{\rm xc}}{\delta \rho(\mathbf{r})} + c_{\rm xc} = \alpha \frac{\delta G_{\rm xc}}{\delta \rho(\mathbf{r})} - c_J \tag{37}$$

where c_J is a large negative value (-5.65 a.u.). So, for the DEKS1 potential to resemble the PBE potential, the term $\alpha \frac{\delta G_{\rm xc}}{\delta \rho(\mathbf{r})}$ needs to incorporate a large negative shift over all of space, compensating for the positive ($-c_J$) shift in Eq (37). This is a severe requirement that is approximately achieved in regions where the density is significant, but cannot be achieved in asymptotic regions because the mathematical form of our $G_{\rm xc}$ yields an asymptotically vanishing potential. The onset of this breakdown is clearly evident at large positive and

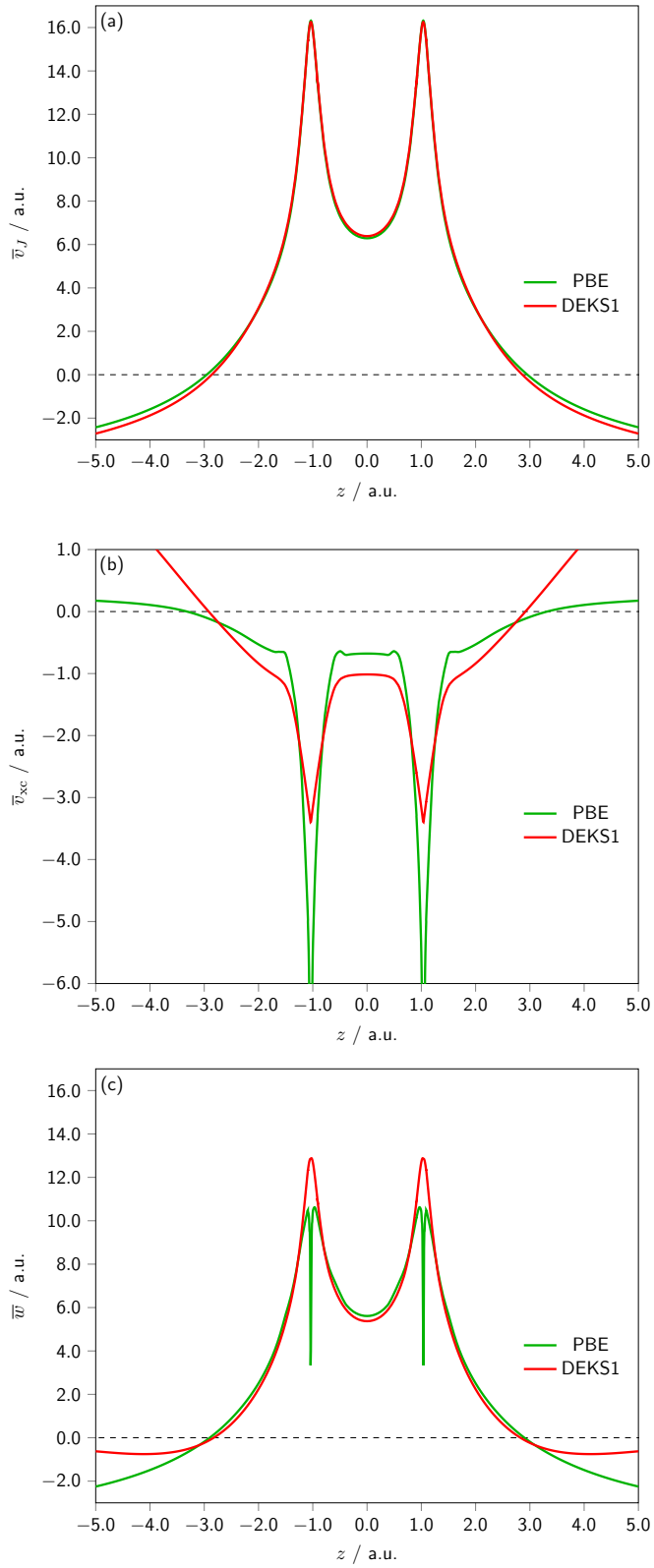

Figure 1: DEKS potentials plotted along the bond axis in N_2, determined using DEKS1 and PBE (in a.u.)

negative z in Figure 1(b), where the DEKS1 potential becomes significantly too positive. The problem can equivalently be phrased in the context of the the total potential, $\overline{w}(\mathbf{r})$: The potential must be shifted from the KS potential by a large, negative value (-5.09 a.u.), but the potential of our approximate G can only introduce a shift in regions where the density is significant; asymptotically, it vanishes, and the onset of this is evident at large and small z in Figure 1(c).

Although we have highlighted this problem for N_2, it will be a problem for all the systems considered, because in all cases the DEKS1 value of c_J is significantly larger in magnitude than the PBE value of $c_{\rm xc}$. (Recall that the average ratio of the quantities is -20.3 for PBE).

3.2 DEKS calculations using $k = 1$ ($c = c_J$, $c_{\rm xc} = 0$)

An obvious way forward is to set $c = c_J$, meaning $c_{\rm xc} = 0$. Eq (37) then becomes

$$\overline{v}_{\rm xc}(\mathbf{r}) = \alpha \frac{\delta G_{\rm xc}}{\delta \rho(\mathbf{r})} + c_{\rm xc} = \alpha \frac{\delta G_{\rm xc}}{\delta \rho(\mathbf{r})} \tag{38}$$

and so $\alpha \frac{\delta G_{\rm xc}}{\delta \rho(\mathbf{r})}$ no longer needs to incorporate a large negative shift over all of space. It simply needs to resemble the PBE KS potential, shifted by its much smaller $c_{\rm xc}$ value. As before, it can only do this in regions where the density is significant, and it will fail asymptotically. But this failure will be less pronounced due to the much smaller magnitude of this shift. In the context of the total potential, setting $c = c_J$ means that we pick up the known, dominant Hartree component of the shift exactly, leaving only a small exchange-correlation component to be recovered by the functional form.

So, for the exchange-correlation part of Hxc, we need a functional for which $c_{\rm xc} = 0$. From Eq (26), this implies

$$E_{\rm xc} = \int v_{\rm xc}(\mathbf{r}) \rho(\mathbf{r}) d\mathbf{r}\,, \tag{39}$$

meaning the exchange-correlation functional must be homogeneous of degree one under den-

sity scaling (see Eq (15)). Note that Eq (39) is a special case ($c_{\text{xc}} = 0$) of Eq (31). We must therefore set $k = 1$ in Eq (19), meaning the Hxc functional is

$$G = J + \alpha\Big(\int \rho^{\frac{3}{2}}(\mathbf{r})d\mathbf{r}\Big)^{\frac{2}{3}}. \tag{40}$$

We then follow the procedure described in Section 2.1, using $c = c_J = -\frac{J}{N}$, $k = 1$, and Eq (21). (In practice, we solve the KS equations (no shift) for the functional and then add the converged value of $c = -\frac{J}{N}$ to each orbital energy at convergence; it is equivalent). The electronic energy in Eq (1) is now equal to the sum of the orbital energies; the maximum discrepancy is $\sim 10^{-5}$ a.u., which arises due to numerical integration / SCF convergence errors. No iterative procedure is required this time, because k has no dependence on the output of the calculation (in contrast to Eq (36) in the DEKS1 case). The results are denoted DEKS2.

Table 1 lists the DEKS2 α values. With increasing N, the values become more negative, but the variation is many orders of magnitude smaller than it was for DEKS1. Tables 2, 3, and 4 list the electronic energies, exchange-correlation energies, and $\overline{\epsilon}_{\text{HOMO}}$ values. Compared to DEKS1, the DEKS2 MADs reduce by more than an order of magnitude for the electronic energy and exchange-correlation energy, and a factor of three for the $\overline{\epsilon}_{\text{HOMO}}$ values. For the electronic energies, essentially exact values can be determined from a knowledge of atomic energies[30] and electronic atomisation energies.[31] Interestingly, the mean absolute deviation of DEKS2 energies from these exact values is just 0.053 a.u., smaller than the PBE deviation of 0.122 a.u. (The DEKS1 deviation is an order of magnitude larger than the DEKS2 deviation).

Figures 2(a), 2(b), and (2c) compare the DEKS2 and PBE DEKS potentials for N_2. The agreement between the Hartree potentials in Figure 2(a) is improved compared to DEKS1; asymptotically, the DEKS2 potential approaches $c_J = -5.23$ a.u., which is now notably closer to the PBE asymptotic value of -5.36 a.u. The improvement in the exchange-correlation

potential in Figure 2(b) is striking; the two curves can barely be distinguished in regions around $z = \pm(0.8 - 1.5)$a.u. This is reflected in the total potential in Figure 2(c), which benefits from a cancellation of errors in asymptotic regions.

As noted above and evident in Figure 2(b), the DEKS2 exchange-correlation potential is unable to reproduce the small positive shift at small and large z, but this is a minor deficiency compared to the DEKS1 case. It is also unable to reproduce the characteristic shell structure in the PBE potential (which is also present in the exact potential, eg see Ref. 32) and this can be traced to the lack of gradient dependence in the functional (as was also observed in Ref. 20). Although there is much room for improvement, the fact that the PBE potential can be reasonably reproduced by the potential of the (unconventional) second term in Eq (40) is intriguing.

3.3 System-dependence of DEKS2 α values and size-extensivity

A drawback of DEKS2 is that the α values in Table 1 were determined from preliminary KS GGA calculations, using Eq (21), meaning DEKS2 calculations cannot be performed without knowledge of an existing exchange-correlation functional (namely PBE). To eliminate this, we must understand the system-dependence of the DEKS2 α values. The following analysis is insightful.

The exchange-correlation functional in DEKS2 is

$$E_{\rm xc} = \alpha\Big(\int \rho^{\frac{3}{2}}(\mathbf{r})d\mathbf{r}\Big)^{\frac{2}{3}}. \tag{41}$$

Consider the application of this functional to a uniform electron gas, where the exchange-correlation energy is approximated by the Dirac exchange energy. Equating the two approximations gives

$$\alpha\Big(\int \rho^{\frac{3}{2}}(\mathbf{r})d\mathbf{r}\Big)^{\frac{2}{3}} = C_{\rm x}\int \rho^{\frac{4}{3}}(\mathbf{r})d\mathbf{r}\,, \tag{42}$$

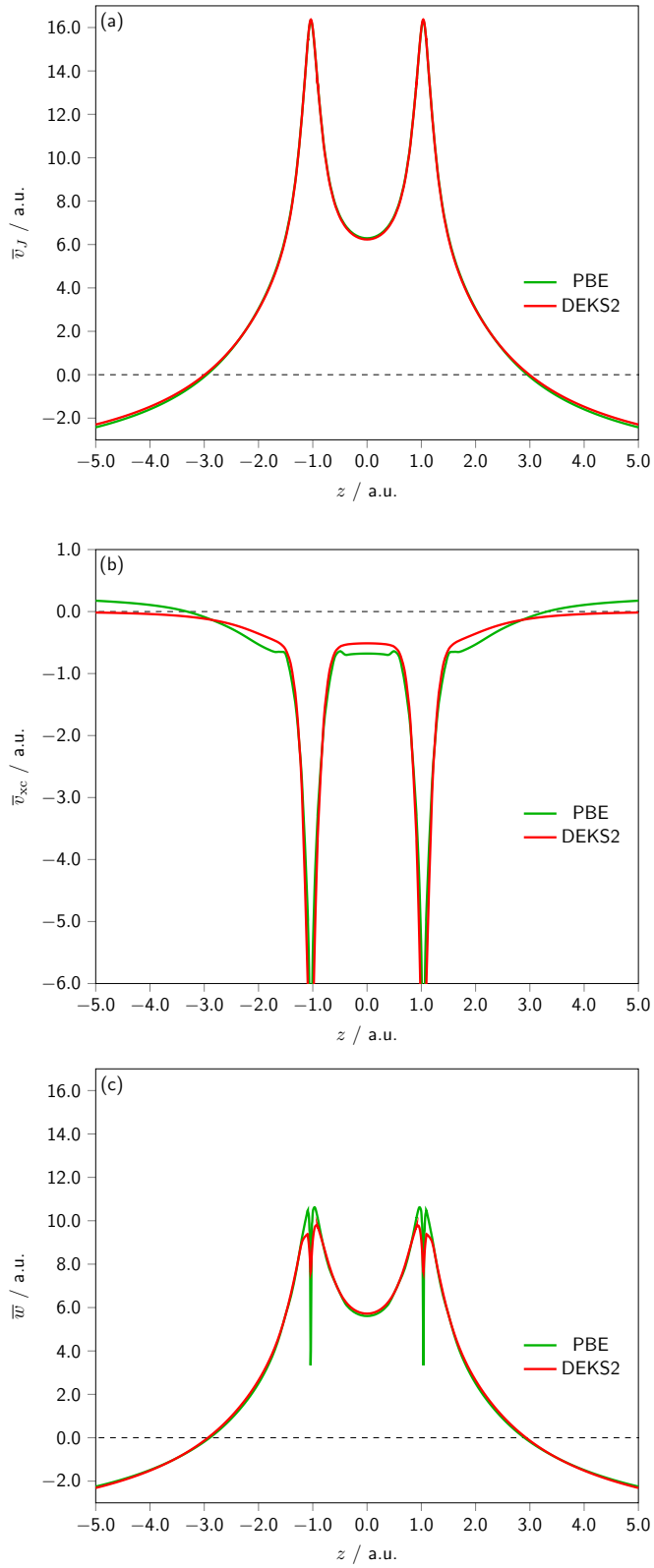

Figure 2: DEKS potentials plotted along the bond axis in N_2, determined using DEKS2 and PBE (in a.u.)

where $C_{\mathrm{x}} = -0.7386$ is the Dirac exchange prefactor.[22] Setting the constant density $\rho(\mathbf{r}) = \frac{N}{V}$, where V is the volume, gives

$$\alpha = C_{\mathrm{x}} N^{\frac{1}{3}} \,. \tag{43}$$

Figure 3 shows a scatter plot of the DEKS2 α values vs $N^{\frac{1}{3}}$ and we do indeed observe a near-linear dependence, consistent with Eq (43). The straight line shown is the best zero-intercept fit, $\alpha = -0.6888 N^{\frac{1}{3}}$ ($R^2 = 0.93$). The prefactor is reassuringly similar to the Dirac value.

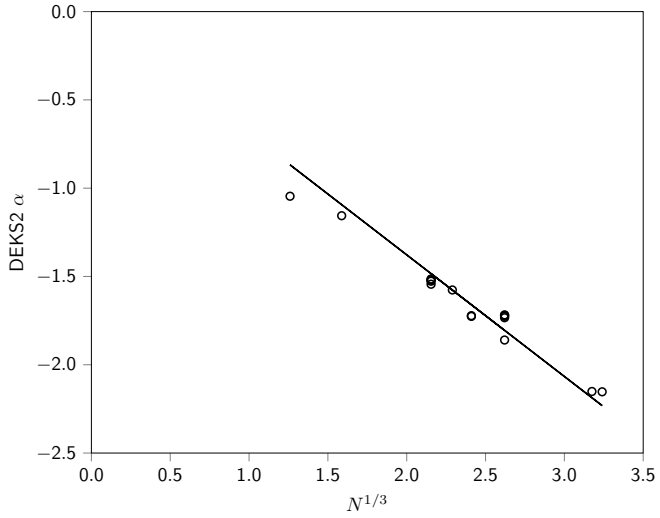

Figure 3: Dependence of the 17 DEKS2 α values on $N^{\frac{1}{3}}$. The straight line is the best zero-intercept fit, $\alpha = -0.6888 N^{\frac{1}{3}}$.

It is pertinent at this point to comment on the issue of size extensivity, which requires the electronic energy of a system composed of two non-interacting closed-shell fragments to equal the sum of the energies of the two fragments.[33,34] If the value of α in Eq (41) was system-*independent* then the presence of the external power differing from unity would mean the functional is not size-extensive, irrespective of whether the two fragments are different or identical. Interestingly, following the above analysis, if we write

$$\alpha = \beta N^{\frac{1}{3}} \tag{44}$$

where β is a system-independent constant, then the functional becomes

$$E_{\rm xc} = \beta N^{\frac{1}{3}} \Big(\int \rho^{\frac{3}{2}}(\mathbf{r}) d\mathbf{r} \Big)^{\frac{2}{3}} , \tag{45}$$

and although this is not size-extensive when the two fragments are different, it is size-extensive when they are identical. Indeed, it yields the correct energy for any number of non-interacting identical fragments due to the cooperativity of the 1/3 and 2/3 powers.

There is a subtle point here. We have chosen to treat N in Eq (45) as a parameter, rather than a functional of the density. By doing this, the desired system-dependence is recovered without affecting the density scaling properties of the functional. If we had instead chosen to treat N as a functional of the density then the desired system-dependence would again be recovered, but the functional would become homogeneous of degree 4/3 (rather than unity) under density scaling. In earlier studies, Parr and Ghosh[35] and Gledhill and Tozer[20] also chose to treat N as a parameter, in the context of the Fermi-Amaldi functional.[36]

3.4 DEKS calculations without preliminary KS calculations

The analysis in Section 3.3 provides a mechanism for eliminating the need for preliminary KS calculations, thereby enabling us to approximate $\overline{w}(\mathbf{r})$ without reference to any existing exchange-correlation functional. We follow the DEKS2 approach with the functional in Eq (40), but rather than evaluating α using Eq (21), we instead use the value in Eq (44), with $\beta = -0.6888$ a.u.. The Hxc functional is therefore

$$G = J + \beta N^{\frac{1}{3}} \Big(\int \rho^{\frac{3}{2}}(\mathbf{r}) d\mathbf{r} \Big)^{\frac{2}{3}} \tag{46}$$

and the shifted potential is

$$\overline{w}(\mathbf{r}) \;\; = \;\; v_J(\mathbf{r}) + \beta N^{\frac{1}{3}} \Big(\int \rho^{\frac{3}{2}}(\mathbf{r}) d\mathbf{r} \Big)^{-\frac{1}{3}} \rho^{\frac{1}{2}}(\mathbf{r}) - \frac{J}{N} \tag{47}$$

(To verify this, substitute for $c = -\frac{J}{N}$, $k = 1$, and $\alpha = \beta N^{\frac{1}{3}}$ in Eqs (22) and (23)). The electronic energy in Eq (1) is again equal to the sum of the orbital energies, to within integration grid / SCF convergence errors. The results are denoted DEKS3.

Table 1 lists the values of $\beta N^{\frac{1}{3}}$, which broadly reproduce the DEKS2 α values. Tables 2, 3, and 4 present the DEKS3 energy quantities. In essentially all cases, the change from DEKS2 to DEKS3 reflects the change in the prefactor: If $\beta N^{\frac{1}{3}}$ is more/less negative than the DEKS2 α value then the energy quantities become correspondingly more/less negative. Overall, DEKS3 cannot compete with DEKS2, but it does perform better than DEKS1 throughout; the $\overline{\epsilon}_{\mathrm{HOMO}}$ values are particularly accurate. Given the simplicity of the potential in Eq (47) and the infancy of the DEKS formalism, we are encouraged by the performance. Indeed, relative to PBE, the DEKS3 electronic energies have a smaller MAD (0.658 a.u.) than that obtained from KS calculations using the S-VWN[22,37] functional (0.929 a.u.), which, like DEKS3, only involves the electron density, with no gradient dependence.

We do not present the DEKS3 potentials for N_2, since on the scale plotted, they are essentially indistinguishable from the DEKS2 potentials in Figure 2. In non-asymptotic regions, the DEKS3 potential is typically 96% of the value of the DEKS2 potential, reflecting the ratio of $\beta N^{\frac{1}{3}}$ to the DEKS2 α value, but this is not visible on the scale plotted.

We make three final remarks. First, by having an explicit functional G, we ensure that the $\mathbf{r}$-dependent part of $\overline{w}(\mathbf{r})$ in Eq (47) is a functional derivative. This is an important condition, which is not necessarily satisfied when a potential is approximated directly, without reference to a functional. Failing to use a functional derivative in KS theory can lead to problems with lack of translational invariance.[38] Second, the fact that we have a functional also means that the approximation in Eq (46) can be used directly in KS theory. Indeed, it may represent a useful research direction in KS theory, independent of the DEKS approach. After all, the only difference between KS and DEKS for this functional is the requirement to add $-J/N$ to the orbital energies in the latter case, before summing them. And third, we comment further on the DEKS3 $\overline{\epsilon}_{\mathrm{HOMO}}$ values in Table 4. The DEKS3 values are in good agreement

with the PBE DEKS values, which themselves have been shown[2,8] to be in rather good agreement with near-exact DEKS values. Of course, neither resemble the negative of the ionisation potential, due to the substantial shifts between the exact DEKS and exact KS HOMO values.

4 Conclusions

DEKS calculations represent a new approach for performing DFT calculations.[2] The central quantity is the shifted Hartree-exchange-correlation potential, $\overline{w}(\mathbf{r})$, which exhibits desirable characteristics, but which must be approximated. We have demonstrated that density scaling homogeneity considerations can be used to facilitate DEKS calculations, providing three approximations to the shifted potential.

DEKS1 calculations using $c = 0$ provide reasonable quality $\overline{\epsilon}_{\mathrm{HOMO}}$ values, suggesting that the shift is successfully incorporated into the potential in regions of space relevant to the HOMO; this was explicitly verified for the N_2 molecule. However, electronic energies and exchange-correlation energies are notably less accurate. Examination of the potentials led us to consider the DEKS2 approach where the dominant Hartree component of the shift is described exactly, using $c = c_J$. This leads to significant improvements, although the results still rely on a preliminary KS PBE calculation for each system. A uniform electron gas analysis was used to eliminate this reliance, enabling us to approximate $\overline{w}(\mathbf{r})$ without reference to any existing exchange-correlation functional. The resulting DEKS3 potential has an unconventional form, Eq (47), which yields encouraging results, intermediate between DEKS1 and DEKS2.

The results of this study provide strong motivation for further research in DEKS theory. We are currently investigating the performance of Eqs (46) and (47) for other molecular properties and we are investigating approaches for further improving accuracy, particularly with regard to the description of the c_{xc} contribution to the shift. The imposition of additional

known exact constraints should help.

5 Acknowledgments

We are grateful to Michael J G Peach for assistance with the production of the figures and to Aron J. Cohen for helpful comments on the draft manuscript.

References

(1) Kohn, W.; Sham, L. J. Self-Consistent Equations Including Exchange and Correlation Effects. *Phys. Rev.* **1965**, *140*, A1133–A1138.

(2) Levy, M.; Zahariev, F. Ground-State Energy as a Simple Sum of Orbital Energies in Kohn-Sham Theory: A Shift in Perspective through a Shift in Potential. *Phys. Rev. Lett.* **2014**, *113*, 113002.

(3) Perdew, J. P.; Parr, R. G.; Levy, M.; Balduz, J. L. Density-Functional Theory for Fractional Particle Number: Derivative Discontinuities of the Energy. *Phys. Rev. Lett.* **1982**, *49*, 1691–1694.

(4) Yang, W.; Zhang, Y.; Ayers, P. W. Degenerate Ground States and a Fractional Number of Electrons in Density and Reduced Density Matrix Functional Theory. *Phys. Rev. Lett.* **2000**, *84*, 5172–5175.

(5) Yang, W.; Cohen, A. J.; Mori-Sánchez, P. Derivative discontinuity, bandgap and lowest unoccupied molecular orbital in density functional theory. *J. Chem. Phys.* **2012**, *136*, 204111.

(6) Sagvolden, E.; Perdew, J. P. Discontinuity of the exchange-correlation potential: Support for assumptions used to find it. *Phys. Rev. A* **2008**, *77*, 012517.

(7) Levy, M.; Zahariev, F. On augmented Kohn–Sham potential for energy as a simple sum of orbital energies. *Mol. Phys.* **2016**, *114*, 1162–1164.

(8) Zahariev, F.; Levy, M. Properties of Augmented Kohn–Sham Potential for Energy as Simple Sum of Orbital Energies. *J. Phys. Chem. A* **2017**, *121*, 342–347.

(9) Vuckovic, S.; Wagner, L. O.; Mirtschink, A.; Gori-Giorgi, P. Hydrogen Molecule Dissociation Curve with Functionals Based on the Strictly Correlated Regime. *J. Chem. Theory Comput.* **2015**, *11*, 3153–3162.

(10) Nazarov, V. U.; Vignale, G. Derivative discontinuity with localized Hartree-Fock potential. *J. Chem. Phys.* **2015**, *143*, 064111.

(11) Nazarov, V. U. Exact exact-exchange potential of two- and one-dimensional electron gases beyond the asymptotic limit. *Phys. Rev. B* **2016**, *93*, 195432.

(12) Davidson, E. R. Selection of the Proper Canonical RoothaanHartreeFock Orbitals for Particular Applications. I. Theory. *J. Chem. Phys.* **1972**, *57*, 1999–2005.

(13) Kaupp, M.; Schleyer, P. v. R.; Stoll, H.; Preuss, H. The question of bending of the alkaline earth dihalides MX2 (M = beryllium, magnesium, calcium, strontium, barium; X = fluorine, chlorine, bromine, iodine). An ab initio pseudopotential study. *J. Am. Chem. Soc.* **1991**, *113*, 6012–6020.

(14) Tozer, D. J. Effective homogeneity of the exchange-correlation energy functional. *Phys. Rev. A* **1998**, *58*, 3524–3527.

(15) Borgoo, A.; Teale, A. M.; Tozer, D. J. Effective homogeneity of the exchange–correlation and non-interacting kinetic energy functionals under density scaling. *J. Chem. Phys.* **2012**, *136*, 034101.

(16) Borgoo, A.; Tozer, D. J. Negative Electron Affinities from DFT: Influence of Asymptotic

Exchange-Correlation Potential and Effective Homogeneity under Density Scaling. *J. Phys. Chem. A* **2012**, *116*, 5497–5500.

(17) Borgoo, A.; Tozer, D. J. Density Scaling of Noninteracting Kinetic Energy Functionals. *J. Chem. Theory Comput.* **2013**, *9*, 2250–2255.

(18) Borgoo, A.; Green, J. A.; Tozer, D. J. Molecular Binding in Post-Kohn–Sham Orbital-Free DFT. *J. Chem. Theory Comput.* **2014**, *10*, 5338–5345.

(19) Borgoo, A.; Teale, A. M.; Tozer, D. J. Revisiting the density scaling of the non-interacting kinetic energy. *Phys. Chem. Chem. Phys.* **2014**, *16*, 14578–14583.

(20) Gledhill, J. D.; Tozer, D. J. System-dependent exchange–correlation functional with exact asymptotic potential and HOMO I. *J. Chem. Phys.* **2015**, *143*, 024104.

(21) Liu, S.; Parr, R. G. Expansions of the correlation-energy density functional $E_c[\rho]$ and its kinetic-energy component $T_c[\rho]$ in terms of homogeneous functionals. *Phys. Rev. A* **1996**, *53*, 2211–2219.

(22) Dirac, P. A. M. Note on Exchange Phenomena in the Thomas Atom. *Proc. Cam. Phil. Soc.* **1930**, *26*, 376–385.

(23) Zhao, Q.; Morrison, R. C.; Parr, R. G. From electron densities to Kohn-Sham kinetic energies, orbital energies, exchange-correlation potentials, and exchange-correlation energies. *Phys. Rev. A* **1994**, *50*, 2138–2142.

(24) Liu, S.; Parr, R. G. Expansions of density functionals in terms of homogeneous functionals:Justification and nonlocal representation of the kinetic energy, exchange energy,and classical Coulomb repulsion energy for atoms. *Phys. Rev. A* **1997**, *55*, 1792–1798.

(25) Levy, M.; Perdew, J. P. Hellmann-Feynman, virial, and scaling requisites for the exact universal density functionals. Shape of the correlation potential and diamagnetic susceptibility for atoms. *Phys. Rev. A* **1985**, *32*, 2010–2021.

(26) Perdew, J. P.; Burke, K.; Ernzerhof, M. Generalized Gradient Approximation Made Simple. *Phys. Rev. Lett.* **1996**, *77*, 3865–3868.

(27) Handy, N. C.; Tozer, D. J. The development of new exchange-correlation functionals: 3. *Mol. Phys.* **1998**, *94*, 707–715.

(28) Amos, R. D.; Alberts, I. L.; Andrews, J. S.; Cohen, A. J.; Colwell, S. M.; Handy, N. C.; Jayatilaka, D.; Knowles, P. J.; Kobayashi, R.; Laming, G. J.; Lee, A. M.; Maslen, P. E.; Murray, C. W.; Palmieri, P.; Rice, J. E.; Simandiras, E. D.; Stone, A. J.; Su, M.-D.; Tozer, D. J. CADPAC 6.5, The Cambridge Analytic Derivatives Package. 1998.

(29) Umrigar, C. J.; Gonze, X. Accurate exchange-correlation potentials and total-energy components for the helium isoelectronic series. *Phys. Rev. A* **1994**, *50*, 3827–3837.

(30) Chakravorty, S. J.; Gwaltney, S. R.; Davidson, E. R.; Parpia, F. A.; p Fischer, C. F. Ground-state correlation energies for atomic ions with 3 to 18 electrons. *Phys. Rev. A* **1993**, *47*, 3649–3670.

(31) Adamo, C.; Ernzerhof, M.; Scuseria, G. E. The meta-GGA functional: Thermochemistry with a kinetic energy density dependent exchange-correlation functional. *J. Chem. Phys.* **2000**, *112*, 2643–2649.

(32) Keal, T. W.; Tozer, D. J. The exchange-correlation potential in Kohn–Sham nuclear magnetic resonance shielding calculations. *J. Chem. Phys.* **2003**, *119*, 3015–3024.

(33) Bartlett, R. J.; Purvis, G. D. Many-body perturbation theory, coupled-pair many-electron theory, and the importance of quadruple excitations for the correlation problem. *Int. J. Quantum Chem.* **1978**, *14*, 561–581.

(34) Helgaker, T.; Jørgensen, P.; Olsen, J. *Molecular Electronic-Structure Theory*; John Wiley & Sons, Ltd, 2000.

(35) Parr, R. G.; Ghosh, S. K. Toward understanding the exchange-correlation energy and total-energy density functionals. *Phys. Rev. A* **1995**, *51*, 3564–3570.

(36) Fermi, E.; Amaldi, E. Le orbite oos degli elementi. *Accad. Ital. Rome* **1934**, *6*, 117–149.

(37) Vosko, S. H.; Wilk, L.; Nusair, M. Accurate Spin-Dependent Electron Liquid Correlation Energies for Local Spin-Density Calculations – A Critical Analysis. *Can. J. Phys.* **1980**, *58*, 1200–1211.

(38) Tozer, D. J. The asymptotic exchange potential in Kohn–Sham theory. *J. Chem. Phys.* **2000**, *112*, 3507–3515.

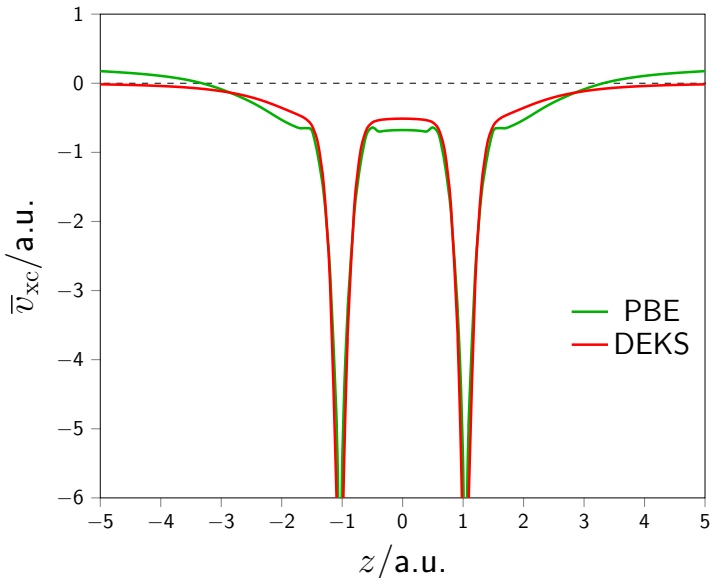

Graphical abstract.